Salient Effects of Bonny Salt Water on The Mechanical Properties of Structures: A Case Study of Automobile Systems

AKPUH DAVIDSON CHIOMA[1], PAUL ABIYE[2], DR. ABDUL MUSA[3], KELECHI UCHENNA UGOJI[4]

[1, 2, 4] *Department of Mechanical Engineering Technology, Federal Polytechnic of Oil and Gas, Bonny*

[3] *Department of Mechanical Engineering Technology, Federal Polytechnic Idah*

Abstract- ***The study investigates the effects of Bonny Island Sailt water on Mechanical Properties of Salt water with emphasis on effectiveness of corrosion prevention methods, specifically nickel electroplating, powder coating, and zinc electroplating, in protecting automotive systems from corrosive environments. Despite its thin coating, nickel electroplating exhibited the highest hardness value and demonstrated superior corrosion resistance in immersion tests, with significantly lower corrosion rates compared to other coatings. Conversely, powder coating, despite having the lowest hardness value, displayed a lower corrosion rate than zinc electroplating, indicating its efficacy as a corrosion prevention method. Tensile tests revealed that mechanical properties such as yield strength and ultimate tensile strength were influenced by specimen preparation and corrosion occurrence. Coated specimens showed varying mechanical properties, with nickel electroplated specimens exhibiting the highest values. Natural water immersion resulted in lower mechanical properties compared to saltwater immersion, suggesting a faster corrosion rate in natural water. Additionally, the study investigates the corrosion resistance of HVOF-coated steels with different compositions. Results indicate that both coatings enhance corrosion resistance compared to untreated steel, with the WC+10%Co+4%Cr coating showing superior performance. These findings suggest that incorporating chromium into the coating composition can significantly improve corrosion resistance in HVOF-coated steels, thus providing effective corrosion prevention in automotive systems exposed to corrosive environments such as Bonny salt water.***

Indexed Terms- ***Bonny Salt Water, Corrosion Rate and Mitigation, Automobile Material Safety and longevity, Environmental Sustainable.***

I. INTRODUCTION

Corrosion, defined as the gradual degradation of materials due to chemical reactions with their surroundings, has been extensively studied and documented with regards automobiles (Borlaug *et al.,* 2018)[1]. A prominent contributor to this corrosion is the presence of salt, especially in the form of road salt used for de-icing in colder regions (Bhattacharyya *et al.,* 2017)[2]. Bonny saltwater, naturally is expected to exist with corrosive properties due to its high salinity content and unique composition.

Corrosion in automobile systems is a multifaceted issue, with implications for both safety and economic considerations. It compromises the structural integrity of critical components in automobile systems (Nascimento *et al*., 2019)[3]. Moreover, it leads to increased maintenance costs, reduced resale value, and environmental concerns, as corroded vehicles may release pollutants and hazardous materials into the environment (Liu *et al.,* 2016)[4]. The economic burden of corrosion in the automobile industry is substantial, estimated to cost billions of dollars annually (Ahammed *et al.,* 2020)[5].

Coastal regions and areas with maritime climates are known for their proximity to bodies of water, such as oceans, seas, and saltwater estuaries (Baker 2017)[6]. These environments are characterized by high levels of humidity and frequent exposure to salt-laden air, creating an ideal setting for accelerated corrosion

processes. Saltwater, in particular, is notorious for its corrosive potential, owing to its high salinity and the presence of dissolved salts, notably chloride ions. The corrosion of automobiles in coastal and maritime environments occurs primarily through electrochemical reactions. Saltwater acts as an electrolyte, enabling the flow of electric current between different metallic components of the vehicle. This process initiates corrosion, leading to the gradual degradation of metal surfaces. It is a self-propagating process, meaning that once corrosion begins, it tends to spread unless mitigated (Nascimento *et al*., 2019)[3].

While road salt is commonly associated with winter road maintenance in colder climates, it is also relevant in the context of saltwater corrosion (Ashraf 2011)[7]. Coastal areas may use salt on roads near the coast to prevent ice formation, introducing additional sources of salt exposure for vehicles. In addition to the corrosive impact of natural saltwater environments in coastal and maritime climates, automobiles are frequently exposed to road salt in regions with colder climates. Road salt, typically in the form of sodium chloride (NaCl) or calcium chloride ($CaCl_2$), is used extensively for de-icing and snow removal on roadways during winter months. While this practice enhances road safety by reducing ice accumulation, it introduces an additional source of salt exposure for vehicles. This exposure can have several adverse effects on the mechanical and structural integrity of automobiles components and metallic structures. The exposure of automobiles to road salt primarily contributes to corrosion through a process known as chemical corrosion. As road salt dissolves, it forms a highly saline solution. This solution can infiltrate various parts of the vehicle, including the undercarriage, wheel wells, and exposed metal surfaces. The chloride ions in the saltwater solution are particularly aggressive when it comes to initiating corrosion. They react with the metal, leading to the breakdown of the passive oxide layer on the surface and promoting further corrosion (Elsener, 2005)[8].

Corrosion necessitates frequent inspections, repairs, and part replacements, all of which contribute to increased maintenance costs for vehicle owners (Danko *et al.,* 2013)[9]. The continual battle against corrosion can strain the financial resources of individuals and organizations. The cumulative effects of corrosion can significantly reduce the overall lifespan of an automobile components and mechanical structures. A vehicle that experiences accelerated corrosion is more likely to be retired from service prematurely, leading to premature depreciation (*Bhattacharyya et al.,* 2017)[2]. Corroded vehicles may release pollutants and hazardous materials into the environment, particularly if corrosion affects components like exhaust systems (Liu *et al.,* 2016)[4]. This can have negative environmental consequences and contribute to air and water pollution.

The presence of corrosion, even if superficial, can negatively impact the resale value of a vehicle. Prospective buyers are often reluctant to purchase vehicles that exhibit signs of corrosion, resulting in decreased resale opportunities (Danko *et al.,* 2013)[7]. Given the importance of automobiles in modern society and the pervasive challenges posed by saltwater corrosion, there is a pressing need to comprehensively understand the effects of saltwater on the mechanical properties of automobile structures. Previous research on corrosion has primarily focused on Corrosion Evaluation of Carbon Steel in Bonny Estuarine Water (Sule *et al* 2020)[10], road salt, leaving a knowledge gap concerning the unique characteristics and effects of natural saltwater environments, such as those encountered in coastal areas like Bonny Island. Thus, this study seeks to address this gap by conducting a detailed investigation into the mechanisms and consequences of Bonny saltwater corrosion on automobile systems.

This research aims to shed light on the salient effects of Bonny saltwater, which may include corrosion rate, variations in mechanical properties, and microstructural changes. This study will provide a comprehensive analysis of the corrosion processes, their impact on structural integrity, and potential strategies for mitigation. Ultimately, the findings of this research will contribute to the development of more robust and corrosion-resistant materials and designs for automobiles, thereby enhancing their reliability and longevity, especially in saltwater-prone regions. In the subsequent sections, this research will delve into the specific objectives,

methodologies, results, discussions, and conclusions derived from this extensive investigation into the salient effects of Bonny saltwater on the mechanical properties of automobile systems.

II. PROBLEM STATEMENT

Corrosive impact of saltwater on the mechanical properties of structures, particularly in automobile systems, presents a significant and multifaceted problem for both the automobile industry and vehicle owners (Okafor and Okoroafor 2019)[11]. While there is a substantial body of research on corrosion-related challenges, including those induced by road salt (Bhattacharyya *et al*., 2017)[2], the specific effects of natural saltwater, such as Bonny Island saltwater, on automobile systems remain inadequately explored. This knowledge gap is a pressing issue given the widespread use of vehicles in coastal and maritime environments.

The existing literature predominantly focuses on the corrosion of automobiles due to road salt and fails to adequately address the unique characteristics and effects of natural saltwater, such as Bonny Island saltwater, which is characterized by its high salinity and specific chemical composition. As a result, there is a notable dearth of knowledge regarding the mechanisms, kinetics, and consequences of corrosion in this context. While corrosion studies exist for various environments, comprehensive data specific to Bonny Island saltwater and its impact on the mechanical properties of automobile systems are scarce. Such data are essential for understanding the extent and severity of corrosion-related issues faced by vehicles components and mechanical structures in coastal regions. Without a clear understanding of the mechanisms involved, it is challenging to design and implement measures to protect vehicles in saltwater-prone environments. In light of these pressing issues and knowledge gaps, this research seeks to comprehensively investigate the salient effects of Bonny saltwater on the mechanical properties of automobile systems. Through laboratory experiments, field studies, and analytical modeling, this study aims to fill the void in the existing literature.

III. LITERATURE REVIEW

Corrosion in automobile systems is a pervasive and complex issue that has far-reaching implications for vehicle safety, performance, longevity, and environmental sustainability. The first point of consideration is the diversity of corrosion types that affect automobiles. These encompass various mechanisms; including uniform corrosion, localized corrosion (such as pitting and crevice corrosion), galvanic corrosion, stress corrosion cracking, and corrosion fatigue (Bhattacharyya *et al.,* 2017)[2]. Each of these mechanisms can target different vehicle components, from external body panels to internal structural elements, electrical systems, and safety-critical parts.

Corrosion in automobile systems poses inherent safety risks. For instance, the corrosion of brake lines or suspension components can lead to catastrophic failures, compromising the vehicle's ability to stop effectively or maintain stability during operation (Heidersbach, *et al*. 2013)[12]. Such safety hazards underscore the critical need to understand and mitigate corrosion in automobile systems and components. Numerous studies have investigated the fundamental corrosion mechanisms in saltwater environment. Cho and Parh (2019)[13] have identified that chloride ion, often abundant in saltwater, play a central role in accelerating corrosion. The extensive research on corrosion mechanisms in saltwater environments has shed light on the critical role of chloride ions and the specific corrosion phenomenon known as pitting corrosion. This understanding is foundational for addressing the challenges posed by saltwater corrosion in various industries, including maritime, oil and gas, and infrastructure development.

The consequences of corrosion in automobile systems extend far beyond mere cosmetic damage; they pose critical safety risks that demand vigilant attention. The most alarming safety hazards arise when corrosion affects vital components such as brake lines and suspension systems. The corrosion-induced deterioration of these components can lead to catastrophic failures, imperiling both vehicle occupants and other road users. The corrosion of brake lines is a particularly perilous consequence of

saltwater exposure and other corrosive environments. Brake lines are responsible for transmitting hydraulic pressure from the brake pedal to the brake calipers, initiating the critical process of stopping the vehicle. When corrosion compromises the integrity of brake lines, they can weaken, develop leaks, or even rupture. This corrosion-induced failure can result in a significant reduction in braking performance, making it difficult for the driver to stop the vehicle promptly and safely (Liu *et al.*, 2016)[4].

Beyond the immediate safety concerns, corrosion in automobile systems carries substantial economic consequences that ripple through the automobile industry and affect individual vehicle owners including mechanical structures. The financial burden imposed by corrosion-related issues encompasses increased maintenance costs, repair expenses, and even premature vehicle replacements. This economic toll underscores the urgency of addressing corrosion to mitigate its impact on both industry and consumers. Corrosion-related maintenance is a continuous and often expensive endeavor. Vehicle owners must contend with frequent inspections, corrosion repairs, and component replacements. Brake lines, exhaust systems, suspension parts, and even body panels may require attention due to corrosion-induced deterioration. These ongoing maintenance expenses can significantly inflate the cost of vehicle ownership over time (Danko *et al*., 2013)[7].

When corrosion progresses to a critical stage, it necessitates not only maintenance but also extensive repairs. For instance, severe corrosion in the undercarriage or frame may demand costly welding and replacement of structural components. Brake system repairs due to corrosion can also be substantial, encompassing the replacement of brake lines, calipers, and rotors. These repair bills add a significant financial burden to vehicle owners and can be unexpected, further straining their budgets. In cases of extensive and irreparable corrosion, vehicle owners may face the need for premature vehicle replacements. This decision often results from the diminishing structural integrity of the vehicle or the uneconomical nature of repairs. Premature replacements disrupt planned vehicle lifespans, forcing owners to incur the significant expense of purchasing a new vehicle sooner than anticipated. For automobile manufacturers, corrosion-related issues can have far-reaching consequences. They may be compelled to address warranty claims and recalls stemming from corrosion-related defects. Such recalls can be not only costly but also damaging to a manufacturer's brand reputation.

The environmental implications of corrosion in automobiles are increasingly recognized. Corroded vehicles may release pollutants and hazardous materials into the environment, contributing to air and water pollution (Mehdizadeh, & Jamal 2017)[14]. Additionally, the disposal of prematurely scrapped vehicles raises concerns related to waste management and resource depletion. One of the primary environmental consequences of corrosion in automobiles is air pollution. Corrosion can lead to the release of particulate matter and chemical compounds from deteriorating components, especially exhaust systems (Liu *et al.*, 2016)[4]. As corrosion progresses in exhaust systems, it can create holes or gaps, allowing unfiltered exhaust gases to escape directly into the atmosphere. These emissions often contain harmful pollutants, including carbon monoxide (CO), nitrogen oxides (NOx), volatile organic compounds (VOCs), and heavy metals like lead and cadmium. These pollutants have adverse effects on air quality, contributing to respiratory diseases and smog formation in urban areas.

Corroded vehicles can also impact water quality. Rainwater washes away corrosion byproducts and surface contaminants from vehicles, transporting them into storm water drains and, ultimately, natural water bodies (Liu *et al*., 2016)[4]. The runoff may contain heavy metals, oil, grease, and other pollutants that pose risks to aquatic ecosystems. In coastal regions or areas near bodies of water, the runoff from corroded vehicles can exacerbate the contamination of marine environments, affecting aquatic life and water quality.

IV. METHODOLOGY

Steel panels were chosen as representative samples of automobile system components due to their high susceptibility to corrosion. These panels are commonly used in various parts of a vehicle,

including the undercarriage, which supports and protects essential components such as the engine, transmission, and exhaust system. Additionally, steel panels are frequently employed in constructing exterior body parts like doors, fenders, hoods, and trunk lids, contributing to the vehicle's aesthetics and offering protection to occupants and internal components. The steel panel samples were selected for uniform composition and sized consistently to Sample parts of automobile parts was initially tested to ascertain their mechanical strengths. The samples was then be immersed in two (2) different water contents. One in Bonny salt water and another in clean water. Both samples was be exposed to rainwater so that whatever effect it has will reflect on both. The clean water content will serve as the control so to speak while the Bonny salt water sample will be our experimental sample. The sample automobile parts was tested periodically for three (3) and the rate of deterioration or weakening of their mechanical strengths ascertain in compliance with Tensile testing (ASTM E8/E8M) and Vicker hardness testing machine was used to ensure accuracy and reliability in testing. Before testing, the specimens were thoroughly cleaned to remove any surface contaminants or existing coatings that might influence the test results. The panels were cut to the required dimensions using precision tools to maintain consistency across all samples. The material utilized for the experiment was a mild steel panel. Mild steel is the most widely used type of steel due to its relatively low cost and acceptable material properties for numerous applications. The composition of the material was analyzed using an Arc Spark Spectrometer

The mounted specimens were then being polished using Polishing machine until they were smooth and shiny before being examined for microstructure and subjected to the Vickers Hardness test. Once the specimens achieved the desired smoothness and shine, they were analyzed for the thickness of the coating. This thickness was measured using a Metallurgical Microscope. The mounted specimen was positioned on the Vickers Hardness Test machine tester. The parameter, namely the load, was set to 100gf. This load was applied to the mounted specimen by the diamond indenter. Following the application of the load, the length of a diagonal of the indentation was measured. Subsequently, the machine generated the hardness value of the specimen, and the hardness reading in HV units was recorded and analyzed.

The immersion corrosion testing method, a conventional approach, was employed to ascertain the weight loss of the metal over a specific duration. This test was conducted in accordance with standard laboratory practices for immersion corrosion testing of metals.

All tests were conducted at room temperature. The test specimen was affixed to the cardboard lid to ensure complete contact with the test solution. The volume of the test solution was sufficient to cover the entire exposed surface of the specimen. Duplicate specimens were utilized for each test category to ensure reliability of the readings. The designated test duration was the maximum period recommended by ASTM, which is 168 hours or 7 days.. The test solution was refreshed daily, and the specimen was cleaned before immersion to maintain consistency. This was repeated for three (3) months on different basis and average values taken. The collected data were then used to calculate the corrosion rate of the metal specimen.

Several steps were taken to execute the immersion corrosion test. The test medium comprised saltwater sourced from Bonny and tap water from the mechanical laboratory. Before commencing the test, the salinity of both the saltwater and tap water was measured using a portable conductivity meter, and the initial weight of the specimen was determined using a weighing machine. Salinity readings were obtained by immersing the sensing rod of the conductivity meter in the medium and stirring until a stable reading was achieved.

Once the salinity was determined, saltwater and tap water were poured into separate 500ml cylinders, and the specimens were immersed in each cylinder, secured with a rope, and labeled accordingly. During the immersion test, the specimens were periodically removed and cleaned to remove corrosion products, employing both chemical and mechanical cleaning methods. After removal from the medium, the specimens were briefly immersed in an acid solution

to remove dirt, followed by brushing to eliminate corrosion. Subsequently, the specimens were weighed to determine the mass loss for each day of immersion, and then returned to the cylinder. The mass loss data for each day were collected for further analysis of the corrosion rate.

Each specimen, after being cleaned with a stiff bristle brush, underwent weighing to determine weight loss during the test. Correction for weight loss resulting from the removal of coating or material surface during the cleaning process was considered. To verify this, one or more cleaned and weighed specimens were subjected to the same cleaning method and re-weighed. The loss observed during this second weighing served as a correction and was subtracted from the total weight loss. Calculation of the corrosion rate necessitates various information and assumptions. It assumes that all mass loss is attributed to general corrosion rather than localized corrosion, such as pitting.

Tensile Test

Following the immersion test, the specimens underwent a tensile test. Conditioning of the specimens was conducted in accordance with ASTM standards. Specifically, ASTM E-8M was employed as the standard for the tensile test. All tests were conducted in a standard laboratory atmosphere with a temperature of 23 ± 2°C and relative humidity of 50 ± 5%. The diagram of the tensile specimen is illustrated in Figure 3.12, while the dimensions of the specimen are provided in Table 3.2 and the material properties are outlined in Table 3.3.

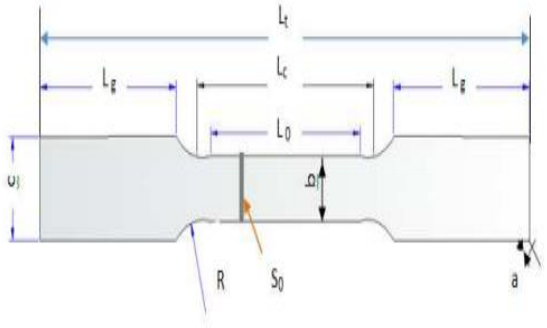

Figure 4.1 Diagram of Tensile Specimen

Table 4.1: Material properties of Specimen at 25°C

Material Grade	Steel panel specimen, cold drawn
Mass density (×1000 kg/m3)	7.87
Modulus of Elasticity (N/mm2)	205000
Poisson's Ratio	0.29
Thermal Coefficient of Expansion (°C -1)	0.0000122

Table 4.2: Dimension of Tensile Specimen

No	Item	Dimensions
1	L_t , Total Length	18.00 cm
2	L_g, Grip Length	5.00cm
3	L_o, Gauge Length	5.5cm
4	L_c, Parallel or reduce Section	6.5 cm
5	R, Radius	1.27 cm
6	a, Thickness	2 mm
7	b, Gauge width	1.25 cm
8	c, Grip width	2.00 cm
9	S_o, Gauge Cross Section Area	25 mm^2
10	A, Total Exposed Surface Area	70.52 cm^2

Figure 4.2: Tensile Strength Testing Apparatus

The tensile test was conducted using a Universal Testing Machine, as depicted in Figure 4.2, in accordance with ASTM test standards. The specimen was positioned vertically in the grips of the testing device. The grips were securely tightened to ensure even and tight gripping and to prevent slippage during the experiment. The specimens were tested at a rate of 2 mm/min, with the testing machine set to the appropriate speed before commencing the test.

V. INSTRUMENTATION

Metallurgical Microscope, Polishing machine, Vickers Hardness Test machine, Universal Testing Machine. Tensile testing (ASTM E8/E8M [1] and the A4 papers, three-in-one computer

VI. CHALLENGES AND LIMITATION

Study of this nature involving management activities, communities and waste like most researches, have its challenges and limitations:

Challenges/Limitations:

- Location: the unfriendly waves of the sea makes ease of transportation both to procure equipment and to assess some needed laboratories outside the island very challenging and risky.
- Accuracy/Measurement: due to the risk or inconveniencing task of handling impact testing and measurements, experiment had to be conducted repeatedly. .
- Maintenance: testing devices/equipment require regular maintenance to ensure accurate readings. Despite these challenges, Researchers ensure maximum possible reliable results.

VII. RESULTS

Table 7.1: The thickness of the different types of coating on the specimens

Type of Coating	Reading 1 (µm)	Reading 2 (µm)	Reading 3 (µm)	Reading 4 (µm)	Reading 5(µm)	Reading Av
Zinc Electroplating	164.7	189.4	203.3	182.8	145.2	177.08
Nickel Electroplating	31.65	31.65	29.15	30.36	30.36	30.63
Powder Coating	194.9	190.0	194.4	192.6	174.5	189.28

The thickness of the coating was being verified under the metallurgical microscope. There were total of 5 points were taken and the average of the thickness was being calculated.

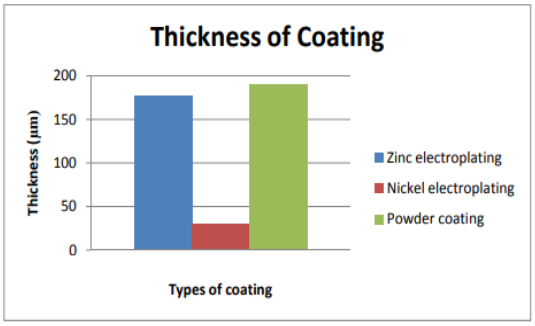

Figure 7.2: Thickness of coating versus types of coating.

Figure 7.1 illustrates the thickness of various corrosion prevention methods applied to the steel panel sample. It is evident that each method resulted in different thicknesses. The average thickness value of the powder coating method is the highest, followed by zinc electroplating, and finally nickel electroplating. Specifically, the average thickness of powder coating reached 189.28µm, the highest among the methods. Conversely, nickel electroplating exhibited the lowest average thickness value of 30.63µm. Zinc electroplating showed an average thickness value of 177.08µm.

Hardness Test

The hardness test was carried out across the small work piece which was being mounted. The tested part was started with the upper coated area to the original steel sample and then to the bottom coated area.

Table 7.2: The hardness value of zinc electroplating versus transverse cross section distance

Zinc Electroplating										
Distance (µm)	60	120	180	200	800	1100	1800	1820	1900	1960
Hardness	27.2	28.4	29.6	233.6	229.1	230.4	229.8	28.7	27.4	25.2 (HV)

Table 7.3: The hardness value of nickel electroplating versus transverse cross section distance

Nickel Electroplating										
Distance (µm)	15	20	25	50	800	1200	1950	1975	1980	1985
Hardness	493.2	483.4	486.9	259.7	248.4	256.7	264.4	486.7	476.9	484.7

Table 7.4: The hardness value of powder coating versus transverse cross section distance

Powder Coating									
Distance (µm)	60	120	180	200	800	1100	1800	1820	1900 1960
Hardness (HV)	9.6	10.4	1	227.4	219.6	216.7	219.1	9.9	8.6 7.4

From the collected data as shown in Table 4.2 to Table 4.4 above, graphs of the hardness versus distance was plotted out for further studies.

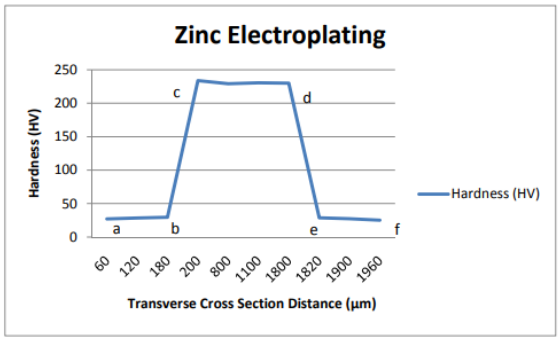

Figure 7.2: Hardness graph (HV) versus Transverse cross section distance (µm) of zinc electroplating.

Figure 7.2 depicts the hardness of the zinc electroplating specimen across different sections: from the coated part to the steel panel and back to the coated part. The figure illustrates that the zinc electroplating part exhibits lower hardness values compared to the steel panel. Initially, the average hardness value of the coated part was 28.4HV. This value sharply increased to an average of 230.73HV at the steel panel. However, the hardness value dropped to an average of 27.1HV at the last section.

The notable disparity in hardness values along the tested part is attributed to the presence of two different materials across the mounted specimens. In summary, the zinc electroplating part shows lower hardness values at both ends of the graph, whereas the steel panel exhibits higher hardness values at the middle of the plotted graph.

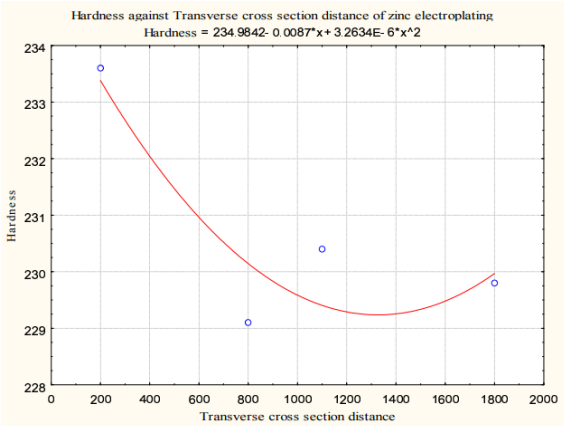

Figure 7.3: Hardness (HV) versus Transverse cross section distance (µm)

The polynomial graph had a mathematical equation of: $234.9842 - 0{,}0087x + 3.2634 \times 10^{-6} - 6x^2$

It shows the minimum graph type because there is dropping of the hardness value when it was tested from the area near the coated part to the steel part.

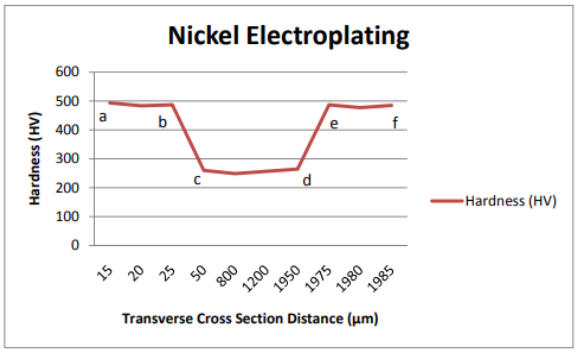

Figure 7.4: Hardness graph (HV) versus Transverse cross section distance (µm) of nickel electroplating.

Figure 7.4 displays the hardness of the nickel electroplating specimen across different sections: from the coated part (a-b) to the steel panel (c-d) and back to the coated part (e-f). The figure illustrates that the nickel electroplating part exhibits higher hardness values compared to the steel panel. Initially, the average hardness value of the nickel electroplating part (a-b) was 487.83HV. This value then decreased to an average of 257.30HV at the steel panel (c-d). Subsequently, the hardness value increased again significantly to an average of 482.77HV at the last section (e-f).

In summary, the nickel electroplating part shows higher hardness values at both ends of the graph, whereas the original steel panel exhibits lower hardness values at the middle of the plotted graph.

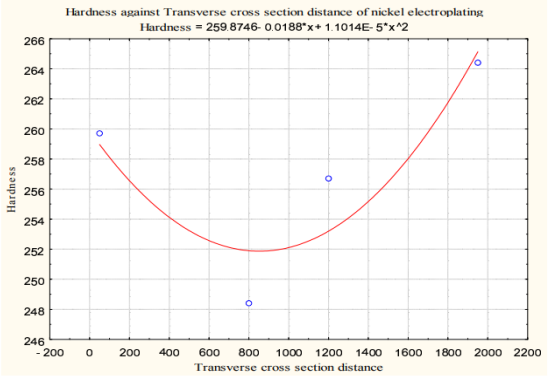

Figure 4.5: Hardness (HV) versus Transverse cross section distance (µm) of the steel panel specimen of the nickel electroplating specimen.

Figure 7.5 shows a polynomial second order of the hardness value (HV) on the steel panel specimen which was tested along the zinc electroplating specimen. The polynomial graph had a mathematical equation of:

$$259.8746 - 0.0188x + 1.1014 \times 10^{-5} - 6x^2$$

It shows the minimum graph type because there is dropping of the hardness value when it was tested from the area near the coated part to the steel panel part.

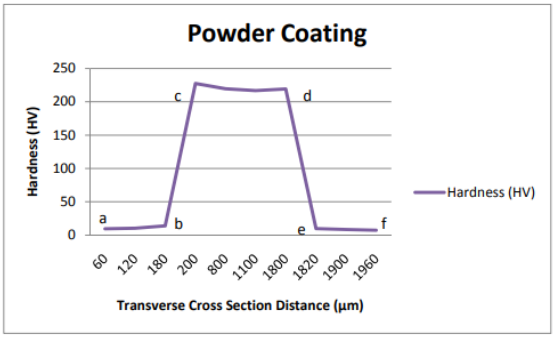

Figure 7.6: Hardness graph (HV) versus Transverse cross section distance (µm) of powder coating.

Figure 7.6 presents the hardness of the powder electroplating specimen across different sections: from the coated part to the steel panel and back to the coated part. The figure indicates that the powder electroplating part exhibits lower hardness values compared to the steel panel. Initially, the average hardness value of the coated part was 11.33HV. This value then sharply increased to an average of 220.70HV at the steel panel. However, the hardness value dropped significantly to an average of 8.63HV at the last section. In summary, the powder coated part shows lower hardness values at both ends of the graph, whereas the steel panel exhibits higher hardness values at the middle of the plotted graph.

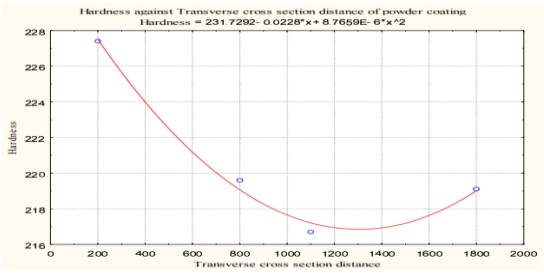

Figure 7.7: Hardness (HV) versus Transverse cross section distance (µm) of the steel panel specimen of the powder coating specimen.

Figure 7.7 shows a polynomial second order of the hardness value (HV) on the steel panel specimen which was tested along the zinc electroplating specimen. The polynomial graph had a mathematical equation of: $231.7292 - 0.0228x + 8.7659 \times 10^{-5} - 6x^2$

It shows the minimum graph type because there is dropping of the hardness value when it was tested from the area near the coated part to the steel panel part.

From the graphs plotted in Figure 4.2 to 4.7, it is noticed that the coating bring a big effect towards the steel sample. Although nickel electroplating has the lowest value in thickness, but it gave the highest hardness value among the three prevention methods applied. For powder coating specimen, it is found that its hardness value is the lowest among the three prevention method. Therefore, it is not suitable to be used for the application to support for high impact.

Corrosion Rate Test

The corrosion rate was being calculated by using the weight loss data taken. The difference weight of the specimens was recorded every day during the immersion test. The net weight loss was gained by using the total weight loss of the specimens minus the total weight loss of the reference specimens. The

Table 4.5 and Table 4.6 was the average net weight loss in salt water and in natural water.

Table 7.8: The average net weight loss on different prevention methods in salt water.

Day	Salt water			
	Zinc	Nickel	Powder	
Without				
	EP	EP	Coating	coating
	Net wt loss (g)	Net wt loss (g)	Net wt loss (g)	Net wt loss (g)
1	0.0536	0.0416	0.0520	0.0685
2	0.0503	0.0015	0.0327	0.0630
3	0.0221	0.0118	0.0238	0.0253
4	0.0071	0.0010	0.0051	0.0092
5	0.0066	0.0035	0.0054	0.0115
6	0.0079	0.0046	0.0053	0.0108
7	0.0433	0.0213	0.0336	0.0550
8	0.0345	0.0110	0.0212	0.0479
9	0.0047	0.0012	0.0024	0.0062
Average	0.02556	0.01083	0.02017	0.03304

Table 7.9: The average net weight loss on different prevention methods in natural water.

Day	Natural water			
	Zinc	Nickel	Powder	
Without				
	EP	EP	Coating	coating
	Net wt loss (g)	Net wt loss (g)	Net wt loss (g)	Net wt loss (g)
1	0.0740	0.0428	0.0505	0.1166
2	0.0757	0.0114	0.0459	0.0779
3	0.0369	0.0172	0.0290	0.0392
4	0.0082	0.0061	0.0072	0.0106
5	0.0079	0.0049	0.0064	0.0187
6	0.0082	0.0059	0.0075	0.0194
7	0.0520	0.0438	0.0544	0.0624
8	0.0487	0.0124	0.0398	0.0539
9	0.0053	0.0023	0.0036	0.0105
Average	0.03430	0.01631	0.02714	0.04547

Table 7.10: The corrosion rate of different types of prevention methods in salt water and natural water

Types of coating	Corrosion Rate (mm/year)	
	Salt water	Natural water
Zinc electroplating	0.01868	0.02506
Nickel electroplating	0.00791	0.01192
Powder coating	0.01474	0.01983
Without coating	0.02414	0.03323

As shown in Table 7.10, the overall corrosion rate in natural water for zinc electroplating, nickel electroplating, powder coating, and uncoated specimens exceeds that of those immersed in salt water by 25.46%, 33.64%, 25.67%, and 27.35%, respectively. This finding contradicts conventional expectations where the corrosion rate in salt water is typically assumed to be higher than that in natural water. This anomaly is attributed to the rapid corrosion of iron or steel when water contains less iron than its maximum solubility.

Table 7.11: Relative corrosion resistance at different range of corrosion rate.

Relative Corrosion Resistance	mpy	mm/yr	µm/yr	nm/yr	pm/yr
Outstanding	<1	<0.02	<25	<2	<1
Excellent	1 – 5	0.02 – 1	25 – 100	2 – 10	1 – 5
Good	5 – 20	0.1 – 0.5	100 – 500	10 – 50	20 – 50
Fair	20 – 50	0.5 – 1	500 – 1000	50 – 150	20 – 50
Poor	50 – 100	1 – 5	1000 – 5000	150 – 500	50 – 200
Unacceptable	200+	5+	5000+	500+	200+

Since the constant K unit was measured in mm/yr, our analysis will primarily focus on the mm/yr column. The results indicate that all coated specimens exhibit corrosion rates within the range of less than 0.2, indicating outstanding corrosion resistance in both salt water and natural water. However, the uncoated specimen shows a corrosion rate falling within the range of 0.02-0.1, which also signifies excellent corrosion resistance. Comparing the corrosion rates of coated and uncoated specimens

in both immersion tests, it's evident that the coated specimens demonstrate lower corrosion rates overall.

Specifically, the data reveals that the nickel electroplating specimen exhibits the lowest corrosion rate, followed by powder coating and zinc electroplating. This suggests that nickel electroplating is the most effective corrosion prevention method among the three tested methods.

Tensile Test

The tensile test was done until the specimen start to fracture and then the value for yield strength and ultimate tensile strength were taken for analysis.

Table 7.12: Data of yield strength and ultimate tensile strength of the specimen before immersion test

Before Immersion		
Test Types of specimen	Yield strength (MPa)	Ultimate tensile strength (MPa)
Without coating	309.9	365.9
Powder coating	317.0	386.2
Zinc electroplating	314.4	379.3
Nickel electroplating	331.5	398.1

The specimen without coating gave the lowest value of the yield strength and ultimate tensile strength, which were 309.9MPa and 365.9MPa. The nickel electroplating specimen has the highest value of ultimate tensile strength and yield strength, which were 398.1MPa and 331.5MPa.

After Immersion Test

The tensile test was then carried out after the immersion test. The first tensile test was carried out after day 2 immersion, followed by day 6 and day 9. The data of yield strength and ultimate tensile strength were recorded and analyzed.

7.13: Yield strength of specimens without coating in salt water and natural water

Yield strength (without coating)				
Day	0	2	6	9
Salt water	309.9	300.4	289.7	287.3
Natural water	309.9	297.5	288.3	279.7

Table 7.14: Yield strength of specimens with powder coating in salt water and natural water

Yield strength (Powder coating)				
Day	0	2	6	9
Salt water	317.0	310.6	306.9	303.2
Natural water	17.0	308.4	302.8	300.6

Table 7.15: Yield strength of specimens with zinc electroplating in salt water and natural water

Yield strength (Zinc electroplating)				
Day	0	2	6	9
Salt water	314.4	303.2	398.8	288.8
Natural water	314.4	298.8	296.3	284.3

Table 7.16: Yield strength of specimens with nickel electroplating in salt water and natural water

Yield strength (Nickel electroplating)				
Day	0	2	6	9
Salt water	331.5	320.6	314.1	303.5
Natural water	331.5	320.0	311.0	301.4

The yield strength of the different types of specimens was recorded as in Table 7.13 to Table 4.16. The data is then used to plot 4 different graphs for further analysis.

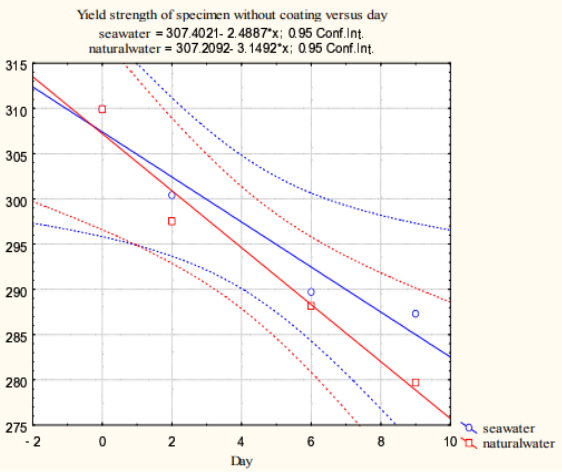

Figure 7.7: Yield strength of specimen without coating versus day

Figure 7.7 shows the yield strength of specimen without coating versus days. The blue line indicated the specimen immersed in salt water whereas the red line indicated the natural water.

Both of the linear line have own mathematical formula, which were 307.4021 – 2.4887X and 301.2092 – 3.1492X for salt water and natural water. The dotted lines show the confidence interval of 95%. The yield strength was decreasing from day 0 to day 9. The initial yield strength recorded was 309.9MPa. By using the mathematical equation, it was found that at day 8, the yield strength of salt water and natural water were recorded as 287.4925MPa and 282.0156MPa respectively. The results show that there was greater dropped in natural water than salt water. There is an intersection point in this graph too. The intersection point shows that the yield strength value is the same for both specimens that immersed in the salt water and natural water on day 0.

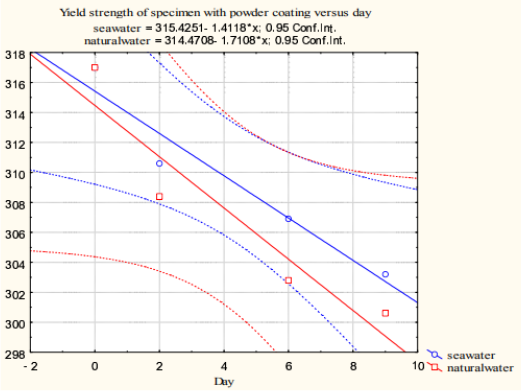

Figure 7.8: Yield strength of specimen with powder coating versus day

Figure 7.8 shows the yield strength of specimen with powder coating versus days. The blue line indicated the specimen immersed in salt water whereas the red line indicated the natural water. Both of the linear line have own mathematical formula, which were 315.4251 – 1.4118X and 314.4708 – 1.7108X for salt water and natural water. The dotted lines show the confidence interval of 95%. The yield strength was decreasing from day 0 to day 9. The initial yield strength recorded was 317.0MPa. By using the mathematical equation, it was found that at day 8, the yield strength of salt water and natural water were recorded as 304.1307MPa and 300.7214MPa respectively. The results show that there was greater dropped in natural water than salt water

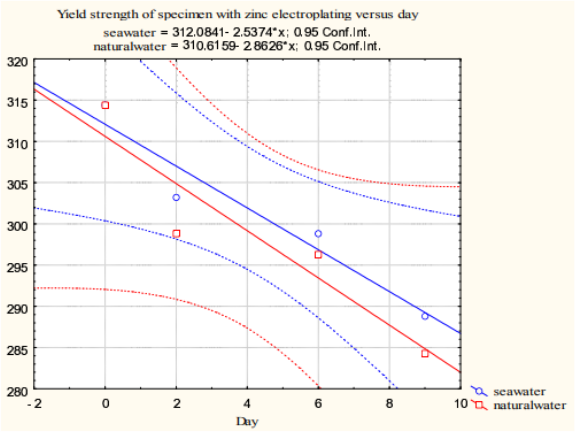

Figure 7.9: Yield strength of specimen with zinc electroplating versus day

The blue line of figure 7.9 indicated the specimen immersed in salt water whereas the red line indicated the natural water. Both of the linear line have own mathematical formula, which were 312.0841 – 2.5374X and 310.6159 – 2.8626X for salt water and natural water. The dotted lines show the confidence interval of 95%. 60 The yield strength was decreasing from day 0 to day 9. The initial yield strength recorded was 314.4MPa. By using the mathematical equation, it was found that at day 8, the yield strength of salt water and natural water were recorded as 291.7849MPa and 287.7151MPa respectively. The results show that there was greater dropped in natural water than salt water.

Figure 4.11 shows the yield strength of specimen with nickel electroplating versus days. The blue line indicated the specimen immersed in salt water whereas the red line indicated the natural water. Both of the linear line have own mathematical formula, which were 329.5364 – 2.8497X and 329.3113 – 3.1379X for salt water and natural water. The dotted lines show the confidence interval of 95%. The yield strength was decreasing from day 0 to day 9. The initial yield strength recorded was 331.5MPa.

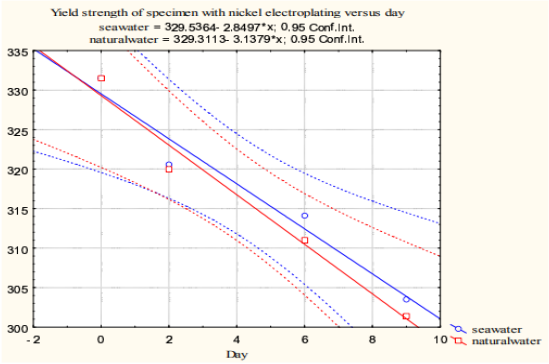

Figure 7.10: Yield strength of specimen with nickel electroplating versus day

By using the mathematical equation, it was found that at day 8, the yield strength of salt water and natural water were recorded as 306.7388MPa and 61 304.2081MPa respectively. The results show that there was greater dropped in natural water than salt water. There is an intersection point in this graph too. The intersection point shows that the yield strength value is the same for both specimens that immersed in the salt water and natural water on day 0. From Figure 7.7 to Figure 7.10, it can be clearly seen that the yield strength of the specimen was decreasing from day 0 to day 9 during the immersion test. The graphs also show that the yield strength of natural water was lower than that in salt water. This outcome depends on the corrosion that happened in two different types of solutions.

Table 7.17 shown the yield strength at day 8 which calculated by using the mathematical equation obtained. The result shows that the specimen with nickel electroplating has the highest value in yield strength, followed by powder coating, zinc electroplating and specimen without coating.

Table 7.17: Yield strength obtained by mathematical equation at day 8

Yield strength (MPa) at day 8		
	Salt water	Natural water
Nickel electroplating	306.7388	304.2081
Powder coating	304.1307	300.7214
Zinc electroplating	291.7849	287.7175
Without coating	287.4925	282.0156

Ultimate Tensile Strength

Table 7.18: Ultimate tensile strength of specimens without coating in salt water and natural water.

Ultimate tensile strength (without coating)				
Day	0	2	6	9
Salt water	367.3	365.9	359.1	350.0
Natural water	367.3	364.2	358.1	348.9

Table 7.19: Ultimate tensile strength of specimens with powder coating in salt water and natural water.

Ultimate tensile strength (Powder coating)				
Day	0	2	6	9
Salt water	386.2	378.8	375.1	370.3
Natural water	386.2	375.2	370.6	368.1

Table 7.20: Ultimate tensile strength of specimens with zinc electroplating in salt water and natural water.

Ultimate tensile strength (Zinc electroplating))				
Day	0	2	6	9
Salt water	379.3	375.9	371.1	369.1
Natural water	379.3	374.8	370.0	367.3

Table 7.21: Ultimate tensile strength of specimens with nickel electroplating in salt water and natural water.

Ultimate tensile strength (Nickel electroplating)				
Day	0	2	6	9
Salt water	398.1	394.9	389.1	378.1
Natural water	398.1	393.4	384.0	372.4

The yield strength of the different types of specimens was recorded as in Table 7.17 to Table 7.21. The data is then used to plot 4 different graphs for further analysis.

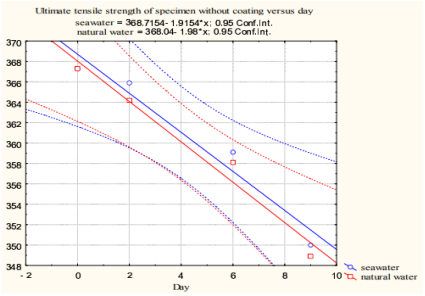

Figure 7.11: Ultimate tensile strength of specimen without coating versus day

Figure 7.11 shows the ultimate tensile strength of specimen without coating versus days. The blue line indicated the specimen immersed in salt water whereas the red line indicated the natural water. Both of the linear line have own mathematical formula, which were 368.7154 – 1.9154X and 368.04 – 1.98X for salt water and natural water. The dotted lines show the confidence interval of 95%. The ultimate tensile strength was decreasing from day 0 to day 9. The initial ultimate tensile strength recorded was 367.3MPa. By using the mathematical equation, it was found that at day 8, the ultimate tensile strength of salt water and natural water were recorded as 353.3922MPa and 352.2MPa respectively. The results show that there was greater dropped in natural water than salt water.

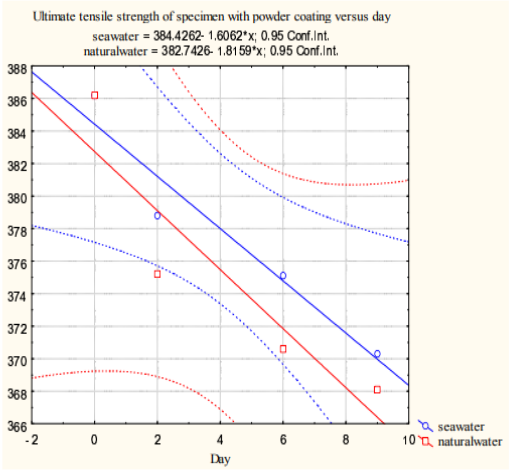

Figure 7.12 Ultimate tensile strength of specimen with powder coating versus day

Figure 7.12 shows the ultimate tensile strength of specimen with powder coating versus days. The blue line indicated the specimen immersed in salt water whereas the red line indicated the natural water. Both of the linear line have own mathematical formula, which were 384.4262 – 1.6062X and 382.7462 – 1.8159X for salt water and natural water. The dotted lines show the confidence interval of 95%. The ultimate tensile strength was decreasing from day 0 to day 9. The initial ultimate tensile strength recorded was 379.3MPa. . By using the mathematical equation, it was found that at day 8, the ultimate tensile strength of salt water and natural water were recorded as 371.5766MPa and 368.2190MPa respectively. The results show that there was greater dropped in natural water than salt water.

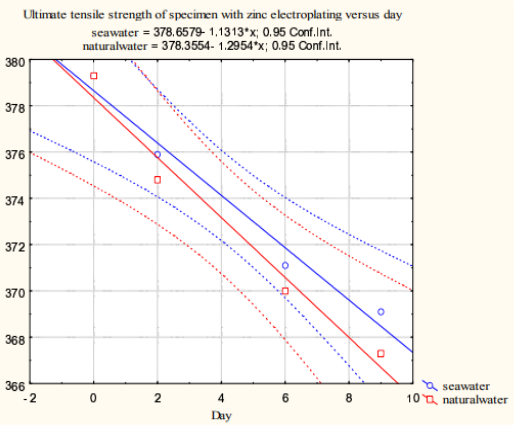

Figure 7.13: Ultimate tensile strength of specimen with zinc electroplating versus day

Figure 7.13 shows the ultimate tensile strength of specimen with zinc electroplating versus days. The blue line indicated the specimen immersed in salt water whereas the red line indicated the natural water. Both of the linear line have own mathematical formula, which were 378.6579 – 1.1313X and 378.3554 – 1.2954X for salt water and natural water. The dotted lines show the confidence interval of 95%. The ultimate tensile strength was decreasing from day 0 to day 9. The initial ultimate tensile strength recorded was 386.2MPa. . By using the mathematical equation, it was found that at day 8, the ultimate tensile strength of salt water and natural water were recorded as 369.6075MPa and 367.9922MPa respectively. The results show that there was greater dropped in natural water than salt water

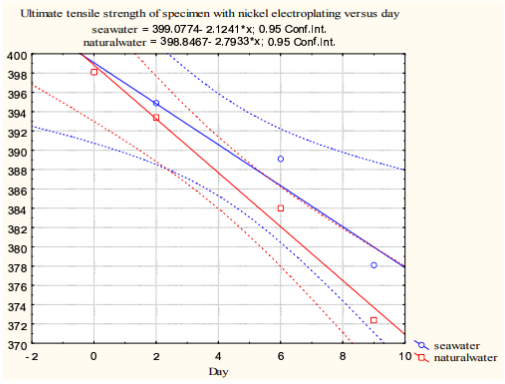

Figure 7.14: Ultimate tensile strength of specimen with nickel electroplating versus day

Figure 7.14 shows the ultimate tensile strength of specimen with nickel electroplating versus days. The blue line indicated the specimen immersed in salt water whereas the red line indicated the natural water. Both of the linear line have own mathematical formula, which were 399.0774 – 2.1241X and 398.8467 – 2.7933X for salt water and natural water. The dotted lines show the confidence interval of 95%. The ultimate tensile strength was decreasing from day 0 to day 9. The initial ultimate tensile strength recorded was 398.1MPa. By using the mathematical equation, it was found that at day 8, the ultimate tensile strength of salt water and natural water were recorded as 382.0846MPa and 376.5003MPa respectively. The results show that there was greater dropped in natural water than salt water. There is an intersection point in this graph. The intersection point shows that the ultimate tensile strength value is the same for both specimens that immersed in the salt water and natural water on day 0.

From Figure 7.12 to Figure 7.15, it can be clearly seen that the ultimate tensile strength of the specimen was also decreasing from day 0 to day 9 during the immersion test as in yield strength graphs plotted. The plotted graphs also show that the ultimate tensile strength of natural water was lower than that in salt water. This condition happened is because the corrosion that happened on the sample specimens has weakened the mechanical properties of the immersed specimens. By using the mathematical equation obtained in each specimen, there was another table that can be generated, as shown in Table 7.19. Table 7.19 shown the ultimate tensile strength at day 8 which calculated by using the mathematical equation obtained. The result shows that the specimen with nickel electroplating has the highest value in ultimate tensile strength, followed by powder coating, zinc electroplating and specimen without coating.

Table 7.22: Ultimate tensile strength obtained by mathematical equation at day 8

Ultimate tensile strength (MPa) at day 8		
	Salt water	Natural water
Nickel electroplating	382.0846	376.5003
Powder coating	371.5766	368.2190
Zinc electroplating	369.6075	367.9922
Without coating	353.3922	352.2000

Results of HVOF Test

Figure 7.15 illustrates the corrosion potential versus time for WC+12Co and WC+10Co+4Cr. Notably, the corrosion potential of the steel (-0.74V) is lower compared to that of the coating-substrate and the coatings themselves. The corrosion process appears to progress more rapidly for the steel in comparison to the coatings, particularly within the range of 0.00 to -0.25 o > -0.50. Consequently, based on this observation and subsequent discussions, it can be anticipated that the corrosion rate of the steel will exceed that of the coated steel.

The behavior of the coated steels falls intermediate to the coating and steel curves, suggesting that both the coating and steel contribute significantly to the corrosion mechanism upon submersion in marine water. Following the corrosion potential test, the presence of iron oxides is evident on the coating surface. This occurrence suggests that the electrolyte can infiltrate the coating pores and interact with the steel substrate. The formation of iron oxide occurs at the coating-substrate interface and emerges on the free surface, indicating a pathway for the iron oxide to exit the interface through the same channels.

An analysis of the coating's free surface after removing the corrosion products reveals a corrosion process involving matrix dissolution into the electrolyte. The WC component remains unaffected, appearing distinct from the matrix that typically encases it, and is observed primarily at the interface between the carbide and matrix. Eventually, the WC undergoes electrochemical attack, leading to its dissolution from the matrix.

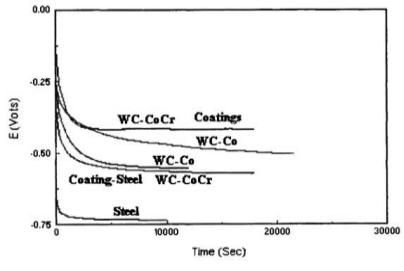

Figure 7.15: Corrosion potential (V) vs. time (s) for the different samples studied.

VIII. DISCUSSION OF RESULTS

The findings of the study reveal that nickel electroplating resulted in the thinnest coating yet possessed the highest hardness value. Moreover, in immersion tests, the nickel electroplated specimen showcased remarkable corrosion resistance, registering the lowest corrosion rate at 0.00791 mm/year in saltwater and 0.1192 mm/year in natural water. Conversely, despite the powder coating specimen exhibiting the lowest hardness value, it demonstrated a lower corrosion rate compared to the zinc electroplated specimen, indicating that powder coating proves to be a more efficacious corrosion prevention method owing to its reduced corrosion rate.

Tensile tests were undertaken to ascertain the yield strength and ultimate tensile strength, crucial mechanical properties significantly influenced by specimen preparation and corrosion occurrence. This underscores the pivotal role of the coating process in mitigating corrosion.

Upon analyzing plotted graphs, a gradual decline in both yield strength and ultimate tensile strength from day 2 to day 9 was observed, attributed to corrosion during immersion tests. Additionally, coated specimens exhibited disparate yield strength and ultimate tensile strength contingent upon the type of coating. Specifically, specimens with nickel electroplating demonstrated the highest values, followed by powder coating, zinc electroplating, and uncoated specimens. Moreover, graphs indicated that specimens immersed in natural water experienced diminished yield strength and ultimate tensile strength compared to those in saltwater, as corrosion advanced more rapidly in natural water. Consequently, specimens immersed in natural water exhibited lower overall yield strength and ultimate tensile strength.

The findings demonstrate the efficacy of coating specimens in delaying corrosion and enhancing mechanical properties in automobile systems. Coatings, particularly nickel electroplating, offer promising solutions for mitigating the detrimental effects of corrosion in saltwater environments. Future research may focus on optimizing coating techniques and exploring alternative materials to further improve corrosion resistance and mechanical performance in automobile applications.

CONCLUSION

This study aimed to investigate the effects of Bonny saltwater exposure on automobile systems, focusing on chemical and electrochemical corrosion processes, corrosion rate following preventive measures, and post-application mechanical characteristics. Through exploration of chemical and electrochemical reactions, it was observed that Bonny saltwater poses significant corrosion risk to automobile systems. Nickel electroplating emerged as a promising corrosion prevention method, exhibiting the highest hardness despite having the lowest coating thickness.

The examination of corrosion rates post-application of preventive measures revealed that nickel electroplating provided the most effective corrosion prevention, exhibiting the lowest corrosion rates in both saltwater and natural water environments. Powder coating also demonstrated superior corrosion resistance compared to zinc electroplating.

Analysis of mechanical characteristics post-exposure to Bonny saltwater indicated a significant impact of corrosion on yield strength and ultimate tensile strength. Corrosion-induced degradation led to a gradual decrease in mechanical properties over the immersion period. Coated specimens, particularly those with nickel electroplating, exhibited higher mechanical strength compared to uncoated specimens, highlighting the efficacy of corrosion prevention techniques in preserving mechanical integrity.

Overall, this study underscores the importance of implementing effective corrosion prevention measures in automobile systems exposed to Bonny saltwater. Nickel electroplating emerged as a promising solution, offering both superior corrosion resistance and mechanical strength. These findings contribute to the advancement of strategies for mitigating the detrimental effects of saltwater exposure on automobile infrastructure, ultimately enhancing durability and reliability in coastal regions.

RECOMMENDATIONS

Based on the findings and discussions presented, the following recommendations are proposed:
Automobile manufacturers and maintenance facilities should prioritize the application of corrosion prevention methods, especially in vehicles operating in coastal regions or areas with high humidity. Nickel electroplating, powder coating, and zinc electroplating have demonstrated effectiveness in delaying corrosion onset and should be considered for application on susceptible automobile components. Regular inspection and maintenance protocols should be established to monitor the condition of coated automobile components and detect signs of corrosion early on. This proactive approach can help identify and address potential corrosion issues before they escalate, thus extending the lifespan of vehicle systems and ensuring safety and reliability. Further research and development efforts should focus on optimizing coating techniques to enhance their effectiveness in corrosion prevention and mechanical strengthening. This may involve exploring advanced coating materials, refining application processes, and conducting thorough performance evaluations under simulated real-world conditions.

Environmental Considerations: When selecting corrosion prevention methods, environmental impact should be taken into account. Manufacturers should prioritize environmentally friendly coating materials and processes that minimize harmful emissions and waste generation. Additionally, efforts should be made to recycle and dispose of coating materials responsibly to minimize environmental footprint.

Training and Education: Training programs and educational initiatives should be developed to raise awareness among automobile professionals about the importance of corrosion prevention and proper coating application techniques. This will help ensure that industry standards are upheld and best practices are followed throughout the manufacturing and maintenance processes.

Continuous Research and Development: Continued investment in research and development is essential to advancing the field of corrosion prevention in automobile systems. Collaborative efforts between industry stakeholders, academia, and research institutions can drive innovation and lead to the development of novel coating technologies with improved performance and durability.

ACKNOWLEDGMENT

Researchers acknowledge the support of Tetfund and Federal Polytechnic of Oil and Gas, who made this study possible. The contributions of colleagues, laboratory staff, students and the Polytechnic host community-Bonny Kingdom is well noted and appreciated.

REFERENCES

[1] Borlaug, G., Jensen, O. M., & Solberg, J. K. (2018). Corrosion of automobile bodies in Norway—measurements and prediction. Corrosion Engineering, Science and Technology, 53(2), 95-102.

[2] Bhattacharyya, S., Pramanik, A., & Sarkar, S. (2017). Environmental effects on corrosion of automobiles: A review. Materials Today: Proceedings, 4(11), 11884-11893.

[3] Nascimento, F. D., Medeiros, A. B., & Rodrigues, J. A. (2019). Corrosion aspects in the automobile industry: An overview. In Handbook of Materials Failure Analysis with Case Studies from the Aerospace and Automobile Industries (pp. 21-49). Woodhead Publishing.

[4] Liu, Y., Zhang, B., & Li, S. (2016). Automobile corrosion: Mechanism, testing, and prevention. In Proceedings of the 9th International Symposium on Advanced Vehicle Control (AVEC'09) (pp. 549-554).

[5] Ahammed, M. M., Pratama, A. P., & Chai, G. B. (2020). Corrosion in the automobile industry: A comprehensive review. Coatings, 10(7), 696.

[6] Baker, D. B. (2017). Road salt impact on freshwater ecosystems: A review. Environmental Pollution, 224, 225-231

[7] Ashraf, M. A., Maah, M. J., & Yusoff, I. (2011). Road salt corrosion and its effect on concrete

properties. Journal of Applied Sciences, 11(16), 2986-2991

[8] Elsener, B. (2005). Chloride-induced reinforcement corrosion: A review. Corrosion Science, 47(1), 1-22.

[9] Danko, M., Karaczun, Z., & Lelito, J. (2013). Effect of deicing agents on the corrosion of car bodies. Archives of Civil and Mechanical Engineering, 13(3), 376-382.

[10] Sule, A. I., Abdullah, M. M. A. B., Annuar, M. S. M., & Abdu, M. (2020). Corrosion Evaluation of Carbon Steel in Bonny Estuarine Water. Journal of Materials Engineering and Performance, 29(12), 8451-8460.

[11] Okafor, P. C., & Okorafor, O. A. (2019). Corrosion of Steel in Tropical Seawater Environment: A Case Study of Bonny River Estuary, Nigeria. Journal of Materials Science Research and Reviews, 4(1), 1-12.

[12] Heidersbach, R. S., Doherty, J. C., & Duncan, M. B. (2013). The effect of road salts on the corrosion of fasteners in a winter maintenance vehicle. Corrosion, 69(8), 854-864

[13] Cho, K., & Park, J. S. (2019). The study on corrosion initiation and propagation of automobiles in salt water immersion condition. Coatings, 9(7), 436.

[14] Mehdizadeh, P., & Jamal, S. (2017). Assessment of corrosion problems in automotive industry. Materials & Design, 120, 236-251